Pergamon

Int. J. Heat Mass Transfer. Vol. 41, No. 12, pp. 1623–1632, 1998

Printed in Great Britain
0017–9310/98 $19.00+0.00

PII: S0017–9310(97)00308–6

Falling film evaporation of single component liquids

ABDULMALIK A. ALHUSSEINI,† KEMAL TUZLA and JOHN. C. CHEN‡

Department of Chemical Engineering, Lehigh University, 111 Research Drive, Bethlehem, PA 18015, U.S.A.

(*Received* 5 *November* 1996 *and in final form* 1 *October* 1997)

Abstract—Heat transfer coefficients for evaporation of single-component liquids in falling films were experimentally measured over an extended range of parameters. By using two different fluids (propylene glycol and water), over a range of absolute pressures, it was possible to extend the existing data base by an order of magnitude in Prandtl numbers. These new data indicate that existing models and correlations were inadequate for fluids with Prandtl numbers greater than five. New models were developed for both the wavy laminar and the turbulent regimes. An exponential interpolation paradigm between the regimes enabled prediction of the evaporative heat transfer coefficient over the entire range of Reynolds and Prandtl numbers with an average deviation of less than 10% from the experimental data. © 1998 Elsevier Science Ltd. All rights reserved.

INTRODUCTION

Falling film evaporators are found in many industrial applications. The inherent advantages of falling thin film flow are short contact time between the process fluid and the heated surface, high heat transfer coefficients, minimal pressure drop, minimal static head, and small process fluid holdup. Short contact time is a key factor when processing heat-sensitive fluids such as in food processing or polymer devolitization. High heat transfer coefficients are always desired, especially in the refrigeration and heat pump applications where significant improvements in cycle efficiency can be achieved by minimizing the temperature difference between the heating medium and the evaporating refrigerant. Minimization of pressure drop is a key advantage when handling viscous liquids as is often the case in the speciality, chemical and polymer industries. Absence of static head minimizes boiling point elevation which is especially important in processes conducted under vacuum conditions. The small process fluid holdup is important when handling environmentally hazardous fluids.

Research on transport phenomena in falling films has ben reviewed by Seban [1] and by Yih [2]. The simultaneous heat and mass transfer in evaporating multicomponent films was studied by Gropp and Schlunder [3], Palen, Wang and Chen [4], Wang [5] and Alhusseini [6]. In the current engineering practice, the mixture heat transfer coefficient is estimated by multiplying a pseudo single component heat transfer coefficient (i.e. calculated from single component correlations using the mixture's physical properties) by a correction factor that accounts for the effects of mass transfer on heat transfer. Therefore, reliable single component heat transfer correlations are very important to the design engineer.

The experimental studies dealing with the evaporation of single component falling films are summarized in Table 1. The most notable of these is the work of Chun and Seban [7] who evaporated water films on an electrically heated vertical tube at atmospheric and vacuum pressures. Reynolds number was varied between 320 to 21 000 to cover both the wavy laminar and turbulent flow regimes. Chun and Seban correlated their data in the wavy laminar region by,

$$h^* \equiv \frac{h(\nu^2/g)^{1/3}}{k} = 0.821 Re^{-0.22} \quad (Re < Re_c) \quad (1)$$

and in the fully turbulent region by,

$$h^* = 0.0038 Re^{0.4} Pr^{0.65} \quad (Re > Re_c). \quad (2)$$

The critical transition Reynolds number was given by: $Re_c = 5900/Pr^{1.06}$ or, $Re_c = 0.215/Ka^{1/3}$. The Chun and Seban correlation currently is widely used in the design of falling film evaporators.

As revealed in Table 1, the existing single component data are limited to a relatively narrow range of physical properties. This is somewhat surprising considering the wide variety of fluids encountered in the applications of falling film evaporators. Prandtl numbers in the prior studies ranged between 1.7 and 5.7, while in applications Prandtl numbers can be order of magnitude greater. Extrapolation of the existing correlations to high Prandtl numbers is not warranted without verification. This study was conducted

†Current address: King Saud University, Chemical Engineering Department, P.O. Box 800, Riyadh 11421, Saudi Arabia.

‡Author to whom correspondence should be addressed.

NOMENCLATURE

A_i^+	a parameter in the free interface eddy viscosity function
A_w^+	a parameter in the wall eddy viscosity function, 26.0
B	coefficient of the free interface boundary layer thermal resistance function
C_r	a term in the approximate expression for h_t^*
g	gravitational acceleration
h	heat transfer coefficient
h^*	dimensionless heat transfer coefficient, $h \cdot l_v/v$
h_l^*	h^* in the wavy laminar region
h_t^*	h^* in the fully turbulent region
k	liquid thermal conductivity
k	Von Karman constant, 0.40
Ka	Kapitza number $(\mu^4 g)/(\rho\sigma^3)$
l_v	viscous length scale $(v^2/g)^{1/3}$
m	exponent of Re in the free interface eddy viscosity function
Pr	Prandtl number, v/α
Pr_t	Prandtl number of turbulence
q	heat flux
Re	film Reynolds number, $4\Gamma/\mu$
T_s	saturation temperature
T_w	wall temperature
u	film's velocity profile
u^+	film's dimensionless velocity profile, u/u^*
u^*	friction velocity $(\delta \cdot g)^{1/2}$
y	distance from the wall
y^+	dimensionless distance from the wall, yu^*/v.

Greek Letters

Γ	liquid mass flow rate per unit flow width
δ	film thickness
δ^+	dimensionless film thickness, $\delta u^*/v$
ε	eddy diffusivity of momentum
ε/v	global eddy viscosity function
$(\varepsilon/v)_i$	dimensionless eddy viscosity function near the free interface
$(\varepsilon/v)_w$	dimensionless eddy viscosity function near the wall
μ	liquid dynamic viscosity
v	liquid kinematic viscosity
π	pi, 22/7
ρ	liquid density
σ	surface tension.

with the following three objectives. First, extend the existing data base for falling evaporation of single component fluids by obtaining experimental data covering a relatively wide range of physical properties. Second, assess the validity of the existing design correlations using the new data. Third, develop improved correlations as necessary.

EXPERIMENT

Heat transfer coefficients for evaporation of single-component films were measured using the facility shown in Fig. 1. The test loop consisted of a vertical evaporator test section, flow recirculation system, and a vacuum system. The test section was an electrically heated stainless steel (SS321) tube of 3.81 cm outside diameter and 3.05 m length. Test liquid was distributed evenly on the external surface at the top of the test tube and flowed down in the form of a falling film. A unique distributor was developed, after multiple bench tests, using a concentric annular port to introduce the liquid as a uniform film around the circumference at the top of the test tube. Electrical heating was supplied by a D.C. rectifier through two electrodes spaced to provide a heated length of 2.90 m. To contain the test fluid (liquid and vapor), the test tube was enclosed within a glass vessel of 15.2 cm diameter along its entire length. The flow recirculation loop consisted to two tanks, a gear pump, a set of flowmeters, two condensers, a cooler, and a preheater. Test liquid exiting at the bottom of the test section was collected in the feed tank while vapor produced in the test section was condensed and remixed with the liquid. Liquid in the feed tank was recirculated by a gear pump to the preheater and brought close to its saturation temperature before being introduced to the top tank, and then distributed as a film over the outside circumference of the test tube.

The vacuum system was used to de-gas the test loop during vacuum operation. The vacuum system consisted of a vacuum pump capable of maintaining 5 mm Hg absolute pressure, two knock-back condensers for recovery of test fluids, a vacuum trap and desiccant bed to protect the vacuum pump. In a typical run, the vacuum line was closed after degassing and pressure inside the test loop was controlled by manipulating the duty of the main condenser.

Type E thermocouples were used to measure temperatures along the adiabatic inner wall of the test tube; these temperatures were then adjusted for gradients through the wall to obtain the external wall temperatures. Nine thermocouple stations with 30.5 cm spacings were located along the test tube. Each station had one thermocouple except the bottom station

Table 1. Experimental studies on falling film evaporation of single component liquids

Authors	Sturve [8]	Elle [9]	Chun and Seban [7]	Fujita and Ueda [10]	Fagerholm *et al.* [11]	Shmerler and Mudawwar [12]	Asblad and Berntsson [13]	Present Study
Year	1969	1970	1971	1978	1985	1988	1991	1995
Heating method	Steam	Electrical	Electrical	Electrical	Hot water	Electrical	Electrical	Electrical
Heated length (m)	1.25	0.975	0.29	0.6–1.0	2.0	0.78	2.16	2.9
Test fluids	R11	R11	Water	Water	R114	Water	R12	Water and propylene glycol
Re range	70–8800	up to 6000	320–21 000	700–9100	up to 11 000	5000–37 500	2000–19 000	34–15 600
Pr range	~4.16	~4.2	1.77–5.7	1.8–2.0	4.8–5.4	1.75–5.4	~3	1.73–46.6
Covered flow regimes	Laminar and turbulent	Turbulent only	Laminar and turbulent	Turbulent only	Turbulent only	Turbulent only	Turbulent only	Laminar and turbulent

which had four thermocouples equally spaced around the circumference to check peripheral uniformity of the film. To insure good contact, the thermocouples were pressed against the test tube's inner wall and were electrically isolated from the test tube by thin fiber glass strips. Other thermocouples were used to measure vapor and liquid temperatures at the inlet and exit of the test section. All thermocouples were wired to read differential temperatures (to improve accuracy), referenced to the measured saturated liquid temperature at the test section exit. Calibration tests indicated an accuracy of better than 1/4°C in differential measurements and 1/2°C in absolute measurements.

An absolute pressure transducer was used to measure pressure at the test section inside the loop. The transducer was accurate to better than one millimeter mercury pressure. Saturation temperatures calculated from pressure measurements and VLE relations agreed within 0.4°C with the measured saturation temperatures. Power measurements were taken by connecting a shunt resistor between the power supply electrodes. Calibration tests confirmed an accuracy of better than 2% in measured power.

A data acquisition system was used to take, store, and display real time measurements for temperatures, pressure, and power. The system consisted of a microcomputer, an eight channel digital data acquisition board with 12 bits accuracy, and a multiplexer board. All data were recorded after attaining steady-state operation. The data was saved on the hard disk for further processing, after taking the average of 100 samples to minimize AC noise.

Water and propylene glycol were used as test fluids in this study. Measurements taken with water provided low viscosity data and helped to establish confidence in our experiment by comparison with previously published water data. With propylene glycol, we were able to obtain measurements at Prandtl numbers close to 50, an order of magnitude greater than the maximum Prandtl number reached in previous studies.

RESULTS

A total of 177 experimental runs were carried out. By adjusting the absolute pressure of the experiments, it was possible to obtain data over an extended range of saturation temperatures and physical properties. Film Reynolds numbers ranged from 124 to 15 600, and the liquid Prandtl numbers ranged from 1.7 to 47. Table 2 shows a list of the operating conditions and range of key variables.

Results are presented in the form of the dimensionless Nusselt number h^*:

$$h^* = h \cdot \frac{l_v}{k} \tag{3}$$

where

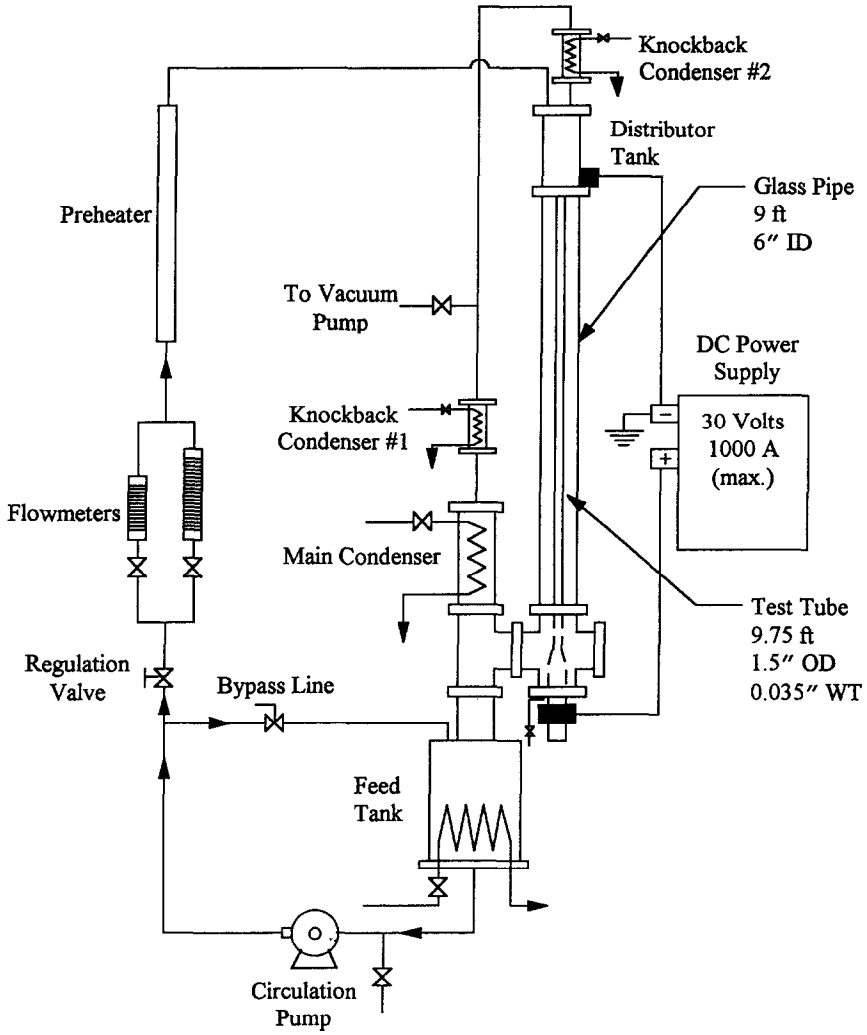

Fig. 1. Test loop schematic.

Table 2. Operating conditions and ranges of key variables

Fluid	T_s (°C)	Heat flux (kW m^{-2})	Reynolds number	Viscosity (centipoises)*	Prandtl number*	Kapitza number*
Water	99.6	18.2	416–15 600	0.28	1.73	1.98×10^{-13}
Water	54.1	19.1	139–8600	0.50	3.22	2.07×10^{-12}
Water	38.5	19.5	190–6527	0.65	4.27	5.15×10^{-11}
Propylene glycol	103.5	7.8	124–1852	2.35	40.2	1.12×10^{-8}
Propylene glycol	94.2	8.04	34–1643	2.85	46.6	2.28×10^{-8}

* Physical properties evaluated at the average film temperature, $T_{av} = (T_w + T_s)/2$.

$$h = q/(T_w - T_s)$$

l_v = viscous length scale

$$= \left(\frac{v^2}{g}\right)^{1/3}.$$

Note that the viscous then scale l_v arises from Nusselt's theoretical analysis for laminar falling films. To determine experimental values of the heat transfer coefficient (h), the surface heat flux (q) was obtained from measurements of electric power input to the test section, and the temperature difference ($T_w - T_s$) was obtained from differential thermocouple measurements. Approximately 100 readings were obtained for

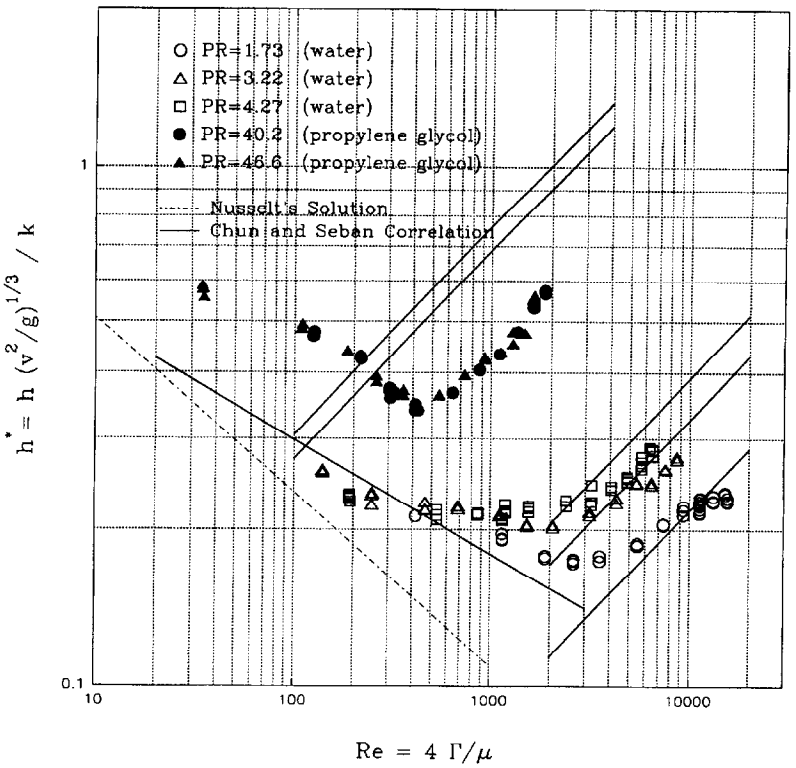

Fig. 2. Measured heat transfer coefficients for water and propylene glycol films compared with Chun and Seban correlation [7].

each parameter, and h calculated as the ratio of time-averaged heat flux and time-averaged temperature difference. The experimental results from the present study are shown in Fig. 2 which plots the nusselt number as a function of film Reynolds number, defined as $4\Gamma/\mu$. General trend of these data is consistent with previous data, showing Nusselt numbers decreasing with increasing Reynolds number for laminar films at low Reynolds numbers. At high Reynolds numbers, turbulent transport dominates leading to increasing Nusselt number with increasing Reynolds number. For a given Prandtl number, the plot of Nusselt vs. Reynolds numbers show a minimum at a critical Reynolds number marking the transition from laminar to turbulent behavior. It is seen that the magnitude of this critical Reynolds number increases with decreasing Prandtl number, varying from 400 to 3000 as Prandtl numbers vary from 47 to 2. This dependence of the critical Reynolds number for transition to turbulence is consistent with suggestions of Chun and Seban [7] and Mudawwar and Elmasri [15].

It is also seen from the results in Fig. 2 that the Nusselt number is parametrically dependent upon the Prandtl number for any given value of the Reynolds number. This Prandtl number dependence has been previously recognized for the turbulent regime and was empirically noted in the Chun–Seban correlation. In the laminar region, previous data with their limited range of Prandtl numbers, did not indicate any parametric effect on h^*. The present data confirms this for Prandtl numbers less than 4.3, but do show a strong parametric effect for higher Prandtl numbers. We believe this is the first reported experimental observation of this behavior in the laminar-film region. This parametric behavior indicates that even in the laminar region, h^* is effected by at least one additional dimensionless parameter besides the Reynolds number. Observation of the laminar film indicates the presence of surface waves which obviously enhances heat transfer beyond that predicted by the Nusselt theory for smooth laminar films. It is reasonable to expect that the extent of wave enhancement is governed by surface, viscous, and body forces—leading to a dependence on a dimensionless parameter in addition to the Reynolds number.

In Fig. 2 the new data are compared to both Nusselt film theory and the well known Chun–Seban correlation. Several observations are noteworthy. First it is seen that data in the laminar film region show higher values for the Nusselt number than that predicted by Nusselt's solution. As noted above, this has been observed by earlier experiments and is commonly ascribed to the enhancement of heat transfer due to surface waves. Second, it is seen that Chun–Seban correlation is in fair agreement with the present data obtained for water, at Prandtl numbers less than 4.3. In this range, the maximum deviation is approximately 30% for both laminar and turbulent regions.

This is a satisfactory result considering the fact that Chun and Seban based their correlation on data obtained with a heated length of only 0.3 m. It is arguable whether such data represent fully developed thermal conditions. Seban and Faghri [16] numerically evaluated turbulent falling films for hydrodynamically developed but thermally non-developed conditions. Their analysis indicated that the Chun and Seban correlation for short heated lengths were approximately 5–20% higher than those calculated for fully developed films. The present experiment utilized a heated length of approximately 3 m, with the data taken at the lowest thermocouple station (corresponding to a heated length of 2.8 m). As shown in Fig. 3, which plots local values of the Nusselt number vs. axial position, these data show little position dependence—confirming fully developed thermal conditions.

The most interesting observations from Fig. 2 is the failure of the Chun–Seban correlation to predict the present data for Prandtl numbers above five. For Prandtl numbers in the range of 40–50, the Chun and Seban correlation under predicts the Nusselt number in the laminar region and over predicts the Nusselt number in the turbulent region, by approximately 50 and 70%, respectively. As noted above, this inadequacy in the laminar region is likely due to unrecognized dependence on surface tension effect. In the turbulent region, it appears that the exponential power of 0.65 on Prandtl number in the Chun–Seban correlation is excessive. It is worth noting that the correlation proposed by Shmerler and Mudawwar [12] has an even larger exponent on the Prandtl number, over predicting the propylene glycol results of this experiment by up to 200%. Based on these new data, it appears that the Prandtl number exponent is more likely in the range of 0.3–0.5, consistent with most turbulent convective transport processes.

ANALYSIS AND DISCUSSION

According to Nusselt's theory, the evaporative heat transfer coefficient for smooth laminar film depends on the following variables,

$$h_N = h_N(\Gamma, \boldsymbol{g}, \rho, \mu, k). \tag{4}$$

By dimensional analysis, it can be shown that,

$$h_N^* \equiv \frac{h_N \cdot l_v}{k} = a \cdot Re^b \tag{5}$$

where a and b are constants. As discussed earlier, heat transfer in wavy laminar films is enhanced by convection induced by large waves that travel along the free surface. Since wave activity is certainly effected by surface tension of the fluid, the heat transfer coefficient in wavy laminar films is expected to depend on σ in addition to the variables in equation (4),

$$h_l = h_l(\Gamma, \boldsymbol{g}, \rho, \mu, k, \sigma). \tag{6}$$

By dimensional analysis, it can be shown that the dimensionless Nusselt number for wavy laminar films should be dependent upon both the film Reynolds number and the Kapitza number where,

$$Ka = \frac{g\mu^4}{\rho\sigma^3}. \tag{7}$$

Ideally one could solve the Navier–Stokes equation for the laminar film including the free surface boundary condition with gravity driven waves. Not having this capability at the present state of CFD devel-

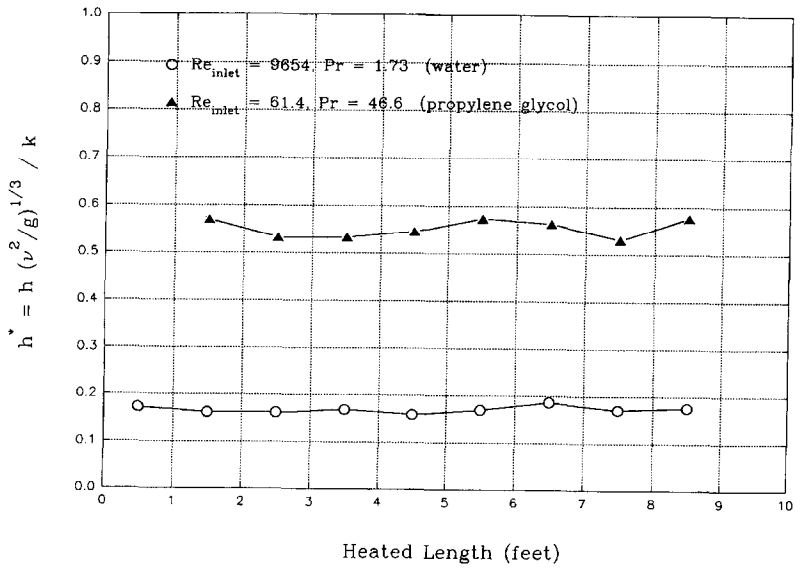

Fig. 3. Axial development of the heat transfer coefficient.

opment, an expedient approach is to seek empirical correlation. Using the new and extended experimental data, together with earlier published data for laminar films, the following dimensionless correlation is proposed for the evaporative heat transfer Nusselt number in the wavy laminar region,

$$h_l^* = 2.65 Re^{-0.158} Ka^{0.0563}. \quad (8)$$

Figure 5 compares this correlation with experimental data; for the laminar region of h^* decreasing with Re, agreement is seen to be reasonable, with an average deviation of less than 10% over the range of Prandtl numbers varying from 1.7–47.

Our effort to model evaporation in the turbulent region consisted of two steps: firstly developing a turbulence model for numerical computation, and secondly obtaining a closed form approximate solution for the dimensionless heat transfer coefficient by asymptotic analysis. In turbulent films evaporating at constant heat flux, the heat transfer coefficient can be calculated by numerically integrating the energy equation as given by,

$$h_t^* = \frac{\delta^{+1/3} \cdot Pr}{\int_0^{\delta^+} \frac{dy^+}{\frac{1}{Pr} + \frac{1}{Pr_t} \cdot \frac{\varepsilon}{\nu}}} \quad (9)$$

where ε is the eddy diffusivity of momentum, ν is the kinematic viscosity, Pr_t is the Prandtl number of turbulence, and y^+ and δ^+ are the dimensionless distance from the wall and film thickness defined as $y^+ = y \cdot u^*/\nu$ and $\delta^+ = \delta \cdot u^*/\nu$ with $u^* = (\delta \cdot g)^{1/2}$. A turbulence model supplies the profiles of the eddy viscosity and Prandtl number of turbulence across the film. Accurate description of the eddy viscosity profile is especially important in predicting the heat transfer coefficient at high Prandtl numbers. The details of the steps taken to develop the turbulence model are discussed by Alhusseini [6]. The model is restricted to cases in which vapor shear at the interface is negligible. An expression is proposed for the eddy viscosity, consisting of two functions. The behavior of the eddy viscosity near the wall and in the core region is expected to be similar to that of conduit flows. In accordance with the treatment by Limberg [22], the mixing length is expressed as a polynomial function of dimensionless distance from the wall. The first function, which accounts for the wall boundary layer and the core region, is given by,

$$\left(\frac{\varepsilon}{\nu}\right)_w = \frac{-1}{2} + \frac{1}{2} \times \sqrt{1 + 4k^2 y^{+2} [1 - \exp(-y^+/A_w^+)]^2 [\exp(-2.5 y^+/\delta^+)]^2} \quad (10)$$

where k is the Von Karman constant and is assigned a value of 0.40 and A_w^+ is assigned a value of 26. For the layer near the free interface, one approach is to

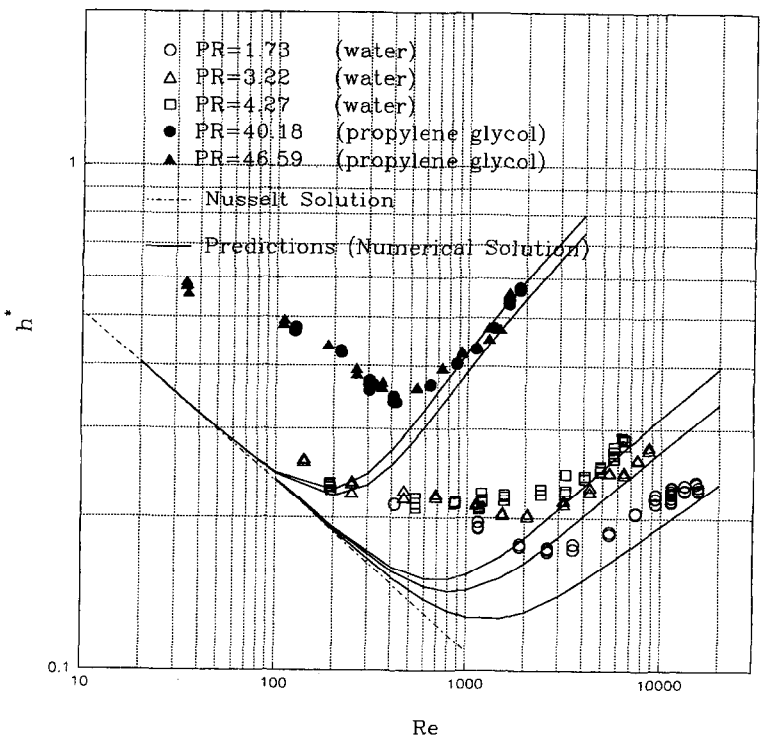

Fig. 4. Comparison of predicted heat transfer coefficients of evaporation using the proposed global eddy viscosity expression, equation (12), with the new evaporation data.

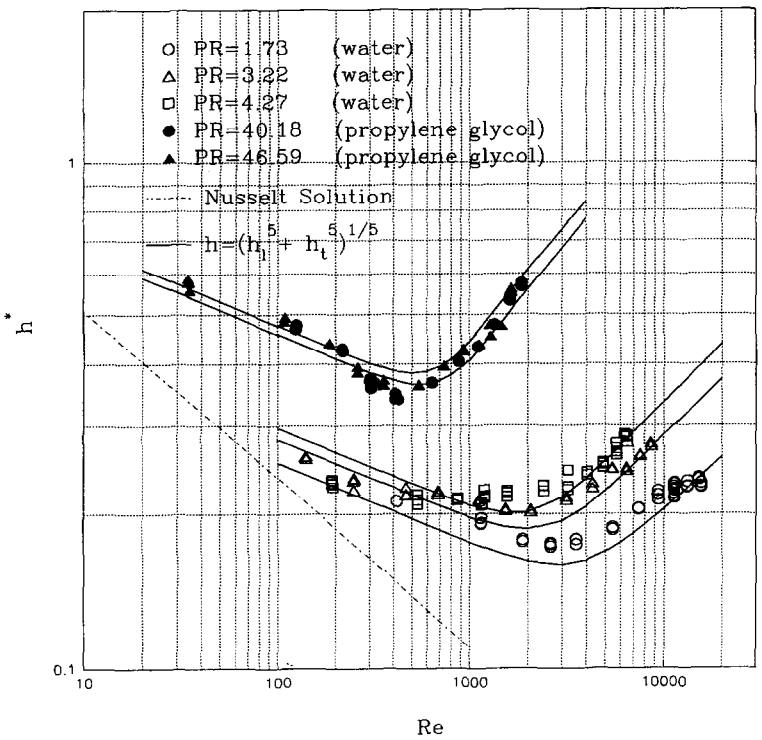

Fig. 5. Comparison of predicted heat transfer coefficient using the proposed combined expression, equation (15), with the new evaporation data.

express the eddy diffusivity by a Taylor series expansion in the dimensionless distance from the free interface. Using the leading term of the expansion, and evaluating the expansion coefficients by comparison with mass transfer data for free surface absorption, from Won and Mills [20], the following second function is obtained to account for the free interface boundary layer,

$$\left(\frac{\varepsilon}{\nu}\right)_i = \frac{1.199\times 10^{-16}}{Ka}\cdot\frac{Re^{2m}}{\delta^{+2/3}}\cdot\left(\frac{Y^+}{A_i^+}\right)^2 \qquad (11)$$

where $m = 3.49Ka^{0.0675}$, $A_i^+ = 0.0166Ka^{-0.1732}$, and δ^+ is calculated from Brauer's turbulent film thickness correlation, $\delta^+ = 0.0946Re^{0.8}$. A global eddy viscosity expression is constructed by taking the lower value of equations (10) and (11),

$$(\varepsilon/\nu) = \text{MINIMUM}\,[(\varepsilon/\nu)_w,(\varepsilon/\nu)_i]. \qquad (12)$$

For the Prandtl number of turbulence, an expression proposed by Kays and Crawford [17] is utilized,

$$Pr_t = \left\{0.581+0.216(\varepsilon/\nu)\,Pr-(0.2(\varepsilon/\nu)\,Pr)^2 \times\left[1-\exp\left(\frac{-1}{0.186(\varepsilon/\nu)\,Pr}\right)\right]\right\}^{-1}. \qquad (13)$$

This expression allows Pr_t to increase near the wall and free interface, which is the expected trend in boundary layers. Equations (9)–(13) together allow numerical calculation of the Nusselt number for evaporating turbulent films.

Since this model concentrates on turbulent films, it can be compared with experimental data at high film Reynolds numbers. In Fig. 4 the ratio of measured to calculated Nusselt numbers are plotted as a function of film Reynold number. The open symbols represent our new data for water at moderate Prandtl numbers and the dark symbols represent new data with propylene glycol at high Prandtl numbers. In the turbulent regime (h^* increasing with Re), the model predicts the new data quite well with an average error less than 10%. The dependence of h^* on Reynolds number and the parametric effect of Prandtl number are well simulated although h^* is slightly underpredicted for the case $Pr = 1.73$. Agreement with data progressively improves as Reynolds number increases, which is expected since the model is valid for fully turbulent films. As Reynolds number is reduced, turbulent activity decays and the predicted h^* goes through a transition region between the fully turbulent and laminar flow regimes. At smaller Reynolds numbers, turbulence is suppressed and the predicted h^* merges with Nusselt's solution for smooth laminar films. This turbulent-transition model can not reproduce the parametric behavior of h^* in the wavy laminar region, since it is based on the smooth film physical model and does not account for enhancement by waves. It is worth noting that the proposed turbulence model is also in good agreement with well known

correlations for the film thickness, heat transfer coefficient for sensible heating, mass transfer coefficients for wall dissolution and mass transfer of absorption for turbulent films.

The second objective here is to obtain a closed form, approximate expression for h_t^* based on the proposed turbulence model. Following an approach similar to that used by Sandall *et al.* [18], an asymptotic expansion of the integral in the energy equation is obtained as fluid Prandtl number (Pr) approached infinity. For this approximate expression, the Prandtl number of turbulence (Pr_t) was assigned a value of 1.1, selected as a reasonable representation of equation (13). The details of this procedure can be found in Alhusseini [6] and are omitted here for brevity. The resulting expression is given by,

$$h_t^* = \frac{Pr \cdot \delta^{+1/3}}{(A_1 Pr^{3/4} + A_2 Pr^{1/2} + A_3 Pr^{1/4} + C_t) + (B Ka^{1/2} Pr^{1/2})} \quad (14)$$

where

$$A_1 = 9.17$$

$$A_2 = 0.328\pi(130 + \delta^+)/\delta^+$$

$$A_3 = 0.0289(152\,100 + 2340\delta^+ + 7\delta^{+2})/\delta^{+2}$$

$$B = 2.51 \times 10^6 \delta^{+0.333} \cdot Ka^{-0.173}/Re^{(3.49 Ka^{0.0675})}$$

$$C_t = 8.82 + 0.0003 Re$$

and

$$\delta^+ = 0.0946 Re^{0.8}.$$

The first term in the denominator of (14) accounts for the thermal resistances of the wall boundary layer and the core region, and the second term accounts for that of the free interface boundary layer. When compared with experimental data for evaporation, the equation proposed by Sandall *et al.* [18] gave good agreement with average deviation of approximately 10%. The expression proposed above, equation (14), improved the agreement further with an average deviation of approximately 6%.

The approximate expression in (14) is a versatile tool because, in addition to predicting the heat transfer coefficient of evaporation, it can also be used to predict the heat transfer coefficient of sensible heating as well as the mass transfer coefficients of absorption, desorption, or wall dissolution. For example, the absorption mass transfer coefficient can be predicted by replacing Pr with Sc and disabling the wall and core resistances, i.e. $A_1 = A_2 = A_3 = C_t = 0$, since the resistance to absorption is mainly due to the free interface boundary layer. For the case of sensible heating, the heat transfer coefficient is predicted by disabling the free interface boundary layer, i.e, $B = 0$, since the resistance is due to the wall boundary layer and, to a lesser extent, the core region. By actual comparison, this model was found to be in very good agreement with Wilke's correlation for the heat transfer coefficient of sensible heating [19], Won and Mills' correlation for the mass transfer coefficient of absorption [20], and Iribarne *et al.* correlation for the mass transfer coefficient of liquid to wall solute transfer [21].

A combined expression for the heat transfer coefficient of evaporation for all Reynolds numbers can be obtained by asymptotic combination of the wavy-laminar and turbulent coefficients,

$$h^* = (h_l^{*5} + h_t^{*5})^{1/5} \quad (15)$$

where h_l^* is the wavy laminar contribution given by equation (8) and h_t^* is the turbulent contribution given by equation (14). As shown in Fig. 5, the combined expression provides a smooth curve in the transition region, and represents the new evaporation data very well over the extended range of Re and Pr.

SUMMARY

New evaporation data were obtained over a Prandtl number range of 1.73–46.6 using water and propylene glycol as test fluids. The new data extended the available data base by an order of magnitude in Prandtl number. The Chun and Seban correlation [7] was found to be inadequate for fluids with Prandtl number larger than five. The experimental Nusselt number h^*, exhibited a parametric behavior in the wavy laminar region which had not been observed heretofore, suggesting that h^* depends on at least one more dimensionless parameter besides Reynolds number. A correlation for h^* in terms of both Reynolds and Kapitza numbers is proposed, for wavy laminar films. A semi-empirical correlation for h^* is proposed for turbulent films. The correlation was found to be in very good agreement with the new evaporation data as well as with well known correlations for heat transfer coefficient of sensible heating and mass transfer coefficients of absorption and liquid to wall solute transfer.

REFERENCES

1. Seban, R. A., Transport to falling films. *Proceedings of the Sixth International Heat Transfer Conference*, Vol. 6. Toronto, Canada (Keynote Paper), 1978, 417–428.
2. Yih, S. M., Modeling heat and mass transport in falling liquid films. *Handbook of Heat and Mass Transfer*, ed. N. P. Cheremisinoff, chap. 5. Gulf Publishing, Houston, Texas, 1986.
3. Gropp, R. and Schlunder, E. U., The effect of liquid-side mass transfer on heat transfer and selectivity during surface and nucleate boiling of mixtures in a film falling film. *Chem. Eng. and Processing*, 1986, **20**, 103–113.
4. Palen, J. W., Wang, Q. and Chen, J. C., Falling film evaporation of binary mixtures. *AICHE Journal*, 1994, **40**(2), 207–214.

5. Wang, Q., Mass transfer effects in falling film evaporation of ternary mixtures, Ph.D. thesis, Lehigh University, Bethlehem, Pennsylvania, 1990.
6. Alhusseini, A. A., Heat and mass transfer in falling film evaporation of viscous liquids, Ph.D. thesis, Lehigh University, Bethlehem, Pennsylvania, 1995.
7. Chun, K. R. and Seban, R. A., Heat transfer to evaporating liquid films. *Journal of Heat Transfer*, 1971, **93,** 391–396.
8. Sturve, H., Der Warmeubergang an einen verdampfenden Rieselfilm. *VDI Forsch. Hft.*, 1969, **534**.
9. Elle, C., Der Warmeubergang bei der Rieselfilm verdampfund des Kaltemittel R11 und Kaltemittles Ol-Gemisches R11-51 KM 33, Thesis, Technischen Universitat, Dresden, G.D.R., 1970.
10. Fujita, T. and Ueda, T., Heat transfer to falling liquid films and film breakdown—II, *International Journal of Heat and Mass Transfer*, 1978, **21,** 109–118.
11. Fagerholm, N. E., Kivioja, K., Ghazanfari, A. R. and Jarvinen, E., An experimental study of heat transfer to falling liquid films. Report No. 3, Institute of Energy Engineering, Helsinki University of Technology, Finland, 1985.
12. Shmerler, J. A. and Mudawwar, I., Local evaporative heat transfer coefficient in turbulent free-falling liquid films. *International Journal of Heat and Mass Transfer*, 1988, **31,** 731–742.
13. Asblad, A. and Berntsson, T., Surface evaporation of turbulent falling films. *International Journal of Heat and Mass Transfer*, 1991, **34,** 835–841.
14. Nusselt, N., Die oberflachenkondenstion der wasserdapfes. *Zeit. Ver D. Ing*, 1916, **60,** 541.
15. Mudawwar, I. and Elmasri, M. A., Momentum and heat transfer across freely-falling turbulent liquid films. *International Journal of Multiphase Flow*, 1986, **12,** 771–790.
16. Seban, R. A. and Faghri, A., Evaporation and heating with turbulent falling liquid films. *Journal of Heat Transfer*, 1976, **98,** 315–318.
17. Kays, W. M. and Crawford, M. E., *Convective Heat and Mass Transfer*, 1st edn, McGraw-Hill, New York, 1980, p. 228.
18. Sandall, O. C., Hanna, O. T. and Ibanex, G. R., Heating and evaporation of turbulent falling liquid films. *AICHE Journal*, 1988, **34,** 502–505.
19. Wilke, W., Warmeugerang an rieselfilme. *Ver Deut Ingr. Forshungsh*, **409**. Dusseldorf, 1962.
20. Won, Y. S. and Mills, A. F., Correlation of the effects of viscosity and surface tension on gas absorption rates in to freely falling turbulent liquid films. *International Journal of Heat and Mass Transfer*, 1982, **25,** 223–229.
21. Iribarne, A., Grossman, A. D. and Spalding, D. B., A theoretical and experimental investigation of diffusion-controlled electrolytic mass transfer between a falling liquid film and wall. *International Journal of Heat and Mass Transfer*, 1967, **10,** 1661–1676.
22. Limberg, H., Warmeubergang an turbulente und laminare rieselfilme. *International Journal of Heat and Mass Transfer*, 1973, **16,** 1696.